J Polym Res (2008) 15:161–171
DOI 10.1007/s10965-007-9155-1

Dynamic mechanical properties of styrene butadiene rubber and poly (ethylene-co-vinyl acetate) blends

C. K. Radhakrishnan · Prajitha Kumari · A. Sujith · G. Unnikrishnan

Received: 15 July 2007 / Accepted: 18 September 2007 / Published online: 13 November 2007

Abstract The dynamic mechanical behaviour of uncrosslinked and crosslinked styrene butadiene rubber/poly (ethylene-co-vinyl acetate) (SBR/EVA) blends was studied with reference to the effects of blend ratio, crosslinking systems, a compatibilizer viz. maleic-anhydride grafted poly [styrene-*b*-(ethylene-co-butylene)-*b*-styrene] (SEBS-g-MA), frequency and temperature. The two separate tan δ peaks, obtained during DMA, indicated the immiscibility of SBR/EVA system. The damping properties increased with SBR content for uncrosslinked and crosslinked blends. In the case of crosslinked systems, depending upon the type of crosslinking agent used, the glass transition temperature (T_g) of SBR phase has been found to be shifted to higher temperatures. The damping characteristics of the blends were observed to be affected by the variations in frequency. The addition of the compatibilizer improved the storage modulus and reduced the damping properties. These results have been correlated with the morphology of the blends, attested by scanning electron micrographs. The activation energy for glass transition has been computed. The experimental data on storage modulus were compared with theoretical predictions.

Keywords Blends · Crosslinking · Compatibilization · Dynamic mechanical analysis · Morphology

Abbreviations

DMA	dynamic mechanical analysis
SEBS-g-MA	maleic anhydride grafted poly (styrene-b-(ethylene-co-butylene)-b-styrene)
E'	storage modulus
E''	loss modulus
E^*	complex modulus
tan δ	dissipation factor
E	activation energy
T	temperature
R	universal gas constant
T_g	glass transition temperature
v	crosslink density
X_C	fractional crystallinity
SEM	scanning electron microscopy
EVA	poly (ethylene-co-vinyl acetate)
SBR	styrene butadiene rubber

C. K. Radhakrishnan (✉) · A. Sujith
Muhammed Abdurahiman Memorial Orphanage College,
Mukkam, Calicut 673602 Kerala, India
e-mail: ckrswathi@yahoo.co.in

P. Kumari · G. Unnikrishnan
National Institute of Technology Calicut,
Calicut 673601 Kerala, India

Introduction

Dynamic mechanical analysis (DMA) has been widely employed for investigating the structure-property relations and viscoelastic behaviour of polymeric materials [1, 2]. The dynamic properties of polymeric materials are of considerable practical significance for several reasons, particularly if they are determined over a wide range of frequencies and temperatures. They can provide insight into various aspects of material structure besides being a convenient measure of polymer transition temperatures. The dynamic properties are of direct relevance to a range of unique polymer applications, concerned with the isolation of vibrations or dissipation of vibrational energy in engineering components [3].

Data obtained from dynamic mechanical testing, over a wide range, can be used to ascertain the molecular response of a polymer in blends with another polymer. In a miscible blend, a single and unique transition will appear, whereas in a highly phase separated polymer blend, the transitional behaviour of the individual components will be unchanged. The viscoelastic properties such as storage modulus, loss modulus and loss

tangent of polymers depend on the structure, crystallinity, extent of crosslinking etc. [4]. Karger-Kocsis and Kiss [5] investigated the morphology and dynamic mechanical properties of polypropylene/ethylene propylene diene terpolymer (PP/EPDM) blends and PP block polymers and reported that an increase in the concentration of EPDM resulted in a decrease in storage modulus (E'). However, these blends are incompatible and have a two-phase morphology evidenced by the presence of two separate damping peaks of blend components remaining at their original positions in the dynamic mechanical spectrum.

Khonakdar et al. [6] studied the miscibility of binary blends of poly (ethylene-co-vinyl acetate) (EVA) with low density polyethylene (LDPE) and high density polyethylene (HDPE) and suggested that DMA was not sensitive enough to study the miscibility of polymer blends with a similar backbone structure. The blends of polyamide (PA6)/ ethylene-butylene elastomer (EB) were subjected to DMA analysis by Omonov et al. [7]. Two characteristic glass transitions were observed for all the blend composition. However the storage modulus of the blends increased with an increase of PA6 content.

The effects of compatibilization on the dynamic mechanical properties of various polymer blends have been reported by several researchers [8–12]. Kader and co-workers [13] studied the morphology and dynamic mechanical behaviour of natural rubber/acrylonitrile-co-butadiene rubber (NR/NBR) blends containing *trans*-polyoctylene rubber as compatibilizer. A reduction in tan δ peak height of NBR and increase in storage modulus have been observed upon compatibilization. The effect of diblock copolymers on the dynamic mechanical properties of polyethylene/ polystyrene (PE/PS) blends has been reported by Brahimi et al. [14]. Their investigations indicated that the addition of pure and tapered diblock copolymers enhanced the phase dispersion and interphase interaction of the blends and that the addition of excess copolymers created micelles. The examination of the compatibility of PC with PS, by Li and Williams [15] using dynamic mechanical measurements, indicated that the system is partially miscible.

Styrene butadiene rubber (SBR) is a general purpose synthetic rubber having high filler-loading, good flex resistance, crack-initiation resistance, and abrasion resistance. However, like other unsaturated rubbers, its ageing resistance is poor, due to the unsaturation in the butadiene component. In order to minimize the oxidative degradation of SBR during service at high at temperature, it is advisable to blend it with a saturated or low unsaturated polymer. EVA copolymer may be considered as a good partner for this purpose because of its excellent ageing resistance, weather resistance, and mechanical properties. In addition, it can provide easier melt processability to the corresponding blends.

The curing behaviour, morphology, mechanical properties, swellings behaviour and ageing characteristics of SBR/EVA blends have been reported by our group earlier [16–18]. These blends were found to be immiscible with low interfacial adhesion between the components. The goal of the present work is to analyze the effects of blend ratio, crosslinking systems and the compatibilizer on the dynamic mechanical behaviour of SBR/EVA blends. The crystallization behaviour of the blends was examined by X-ray scattering.

Experimental

Materials

Styrene-butadiene rubber (SBR) marketed under the trade name Syanaprene (SBR-1502) was obtained from Korea Kumho Petrochemical Co., Ltd (Ulsan, Korea). Poly (ethylene-co-vinyl acetate) (EVA) used was EVA-1802 obtained from National Organic and Chemical Industries Ltd. Mumbai, India. The basic characteristics of SBR and EVA are given in Table 1. The compatibilizer used was maleic-anhydride grafted poly[styrene-*b*-(ethylene-co-butylene)-*b*-styrene](SEBS-g-MA) triblock copolymer, Kraton FG1901X, supplied by Shell Chemicals, Houston, Texas, USA, having 29% styrene and 1.84% grafted maleic anhydride. The rubber chemicals used such as sulphur, dicumyl peroxide, zinc oxide, stearic acid, and mercapto benzothiazyl disulphide (MBTS) were of commercial grade.

Blend preparation

The blends of SBR and EVA were prepared, on a laboratory type (150 mm×300 mm) two roll mixing mill having a friction ratio of 1:1.4, as per ASTM D-15-627. Initially SBR and EVA were separately masticated. The masticated rubbers were then blended together and compounded. The temperature of the rollers of the mill was kept at 70 °C. Uncrosslinked blends were compression moulded at 150 °C. The different crosslinking systems used viz. sulphur (*S*), dicumyl peroxide (DCP) and mixed (*S*+DCP) have been indicated as *S*, *P* and *M* respectively. The compounds having sulphur system are designated as S_0 (pure SBR), S_{20} (80/20 SBR/EVA), S_{40} (60/40 SBR/EVA) and so on. Similarly, the compounds with peroxide and mixed curing systems are designated respectively as P_0 and M_0 (pure SBR), P_{20} and M_{20} (80/20 SBR/EVA), P_{40} and M_{40} (60/40 SBR/EVA) and so on. The subscripts indicate the weight percentage of EVA in the blends. S_{100} and M_{100} samples could not be moulded, probably due to the saturated backbone of EVA. The compatibilizer, SEBS-g-MA used in this study, has been coded as *C*. The compatibilizer loading has been indicated by a subscript. For instance $P_{60}C_6$ indicates peroxide cured

Table 1 Details of materials

Materials	Characteristics		Source
Styrene butadiene rubber (SBR-1502)	Styrene content (%)	24.000	Korea Kumho Petrochemicals Co. Ltd. Korea
	Volatile matter (%)	0.750	
	Organic acid	4.750	
	Soap	0.500	
	Ash	1.500	
	Antioxidant	0.500	
	Density (kg/m^3)	940.000	
	Mooney viscosity (ML $_{1+4}$; 100 °C)	46.000	
Poly (ethylene-co-vinyl acetate) (EVA-1802)	Melt flow index (kg/10 min)	0.002	
	Density (kg/m^3)	940.000	National Organic and Chemical Industries Ltd., Mumbai, India
	Vicat softening point (°C)	59.000	
	Vinyl acetate (%)	18.000	
	Intrinsic viscosity (dL.g)	0.170	

40/60 SBR/EVA blend containing 6 phr of the compatibilizer and $S_{60}C_6$ indicates sulphur cured 40/60 SBR/EVA blend containing 6 phr of the compatibilizer. The compounding recipes of the blends are given in Table 2. The compounded blends were compression moulded at 160 °C under a pressure of 6.7 MPa, for the optimum cure.

Morphological studies

The samples for SEM studies were cryogenically fractured and the surface was treated with osmium tetroxide (OsO_4) for 10 min in order to stain selectively the unsaturated SBR phase. These samples were sputter coated with gold and SEM examinations were performed on a Cambridge Instrument (S360). Morphology of the blend systems has also been studied by using an optical microscope (Leica Microsystem, Wetzer, Germany). For this, 5% solutions of SBR and EVA with varying proportions were prepared in chloroform. They were stirred for 36 h using a magnetic stirrer and then solution casted as thin films of 20 μm thickness. Photomicrographs of the samples in the transmission mode with cross-polarized light and day light filter were taken.

Table 2 Formulation of the mixes (phr)

Ingredients (phr)	Sulphur system	Peroxide system	Mixed system
Polymer	100	100	100
Zinc oxide	4	–	4
Stearic acid	2	–	2
[a]MBTS	1.5	–	1.5
Sulphur	2	–	2
Dicumyl peroxide	–	4	4

[a] Mercaptobenzothiazyl disulphide.

Dynamic mechanical analysis (DMA)

Dynamic mechanical properties of the blends were investigated by using a dynamic mechanical analyzer Netzsch DMA 242 (Germany) at different frequencies (0.1, 1, 10 and 50 Hz). The experiments were conducted in bending mode at an amplitude of 50 μm. Liquid nitrogen was used to achieve sub-ambient temperatures and a programmed heating rate of 3 °C min^{-1} was given. The test specimens were of length – 55 mm, width – 5 mm and thickness – 2 mm. The analysis was carried out over a temperature range of −100 to 120 °C. The storage modulus E', loss modulus E'' and the

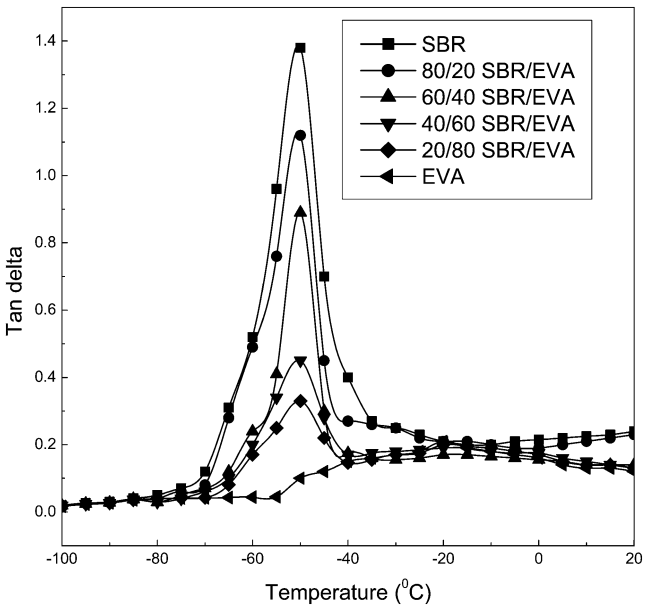

Fig. 1 Damping properties of uncrosslinked SBR/EVA blends as a function of blend ratio and temperature (−100 to 20 °C) at a frequency of 1 Hz

mechanical loss factor tan δ have been obtained from the following equations,

$$E'' = E^* \sin\delta \quad (1)$$

$$E' = E^* \cos\delta \quad (2)$$

where E^* is the dynamic complex modulus
The loss tangent has been computed as:

$$\tan\delta = E''/E' \quad (3)$$

X-ray studies

In order to find out the degree of crystallinity of different blends, X-ray diffraction patterns of the samples were recorded using an X-ray diffractometer with Ni-filtered CuK_α radiation from a Bruker D8 instrument. The angular range was 5 to 40° (2θ). Samples having same thickness and area were exposed to the X-ray source. The operating voltage and the current of the tube were kept at 40 kV and 20 mA, respectively, throughout the experiments.

From the X-ray diffraction pattern, the areas under the crystalline (I_c) and amorphous portions (I_a) were measured in arbitrary units and the degree of crystallinity (X_c) of the samples was calculated as,

$$X_C = \frac{I_c}{I_c + I_a} \quad (4)$$

where I_c and I_a represent the integrated intensities corresponding to the crystalline and amorphous phases respectively, i.e., the area under the respective curves.

Results and discussion

Effect of blend composition

The loss-tangent (tan δ) values of the component copolymers and the uncrosslinked blends at 1 Hz as a function of

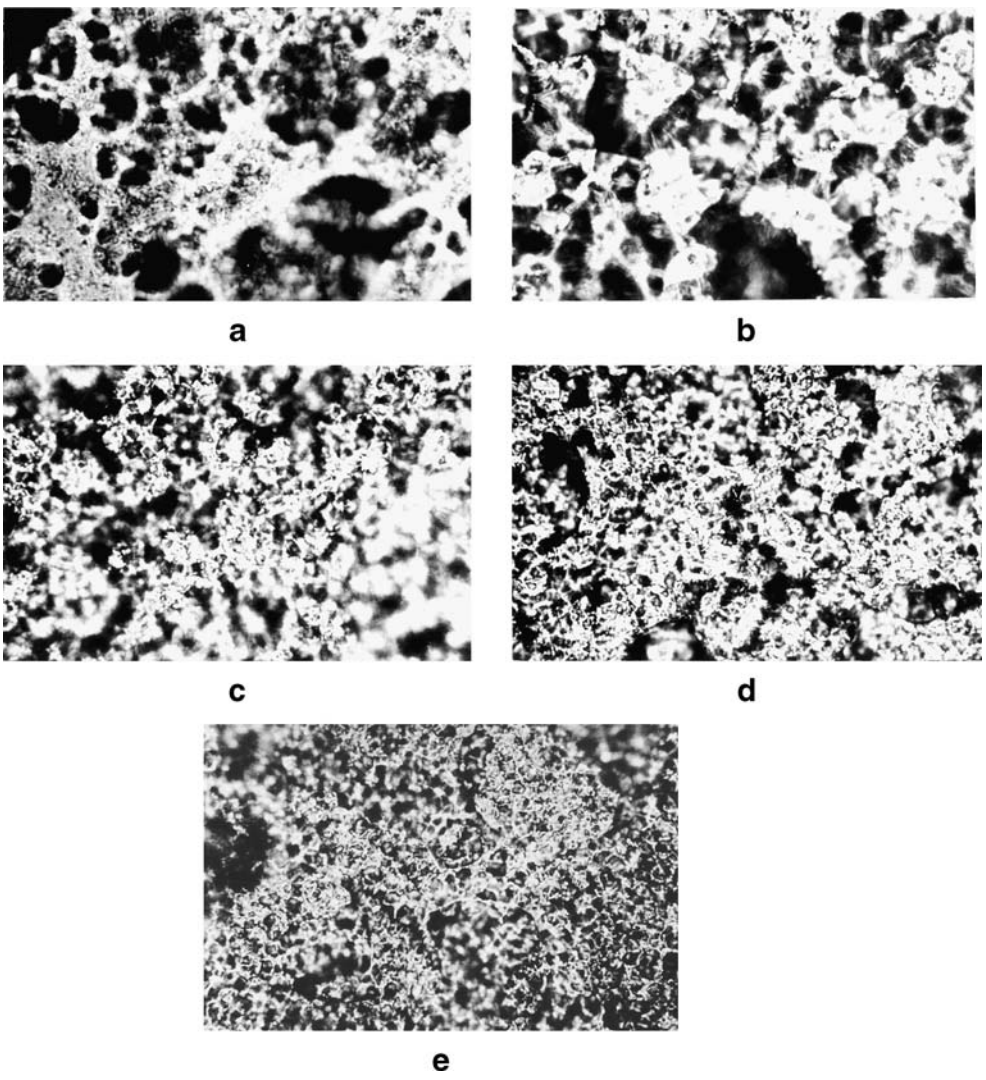

Fig. 2 Optical micrographs showing the morphology of (**a**) 80/20 SBR/EVA (**b**) 60/40 SBR/EVA (**c**) 50/50 SBR/EVA (**d**) 40/60 SBR/EVA and (**e**) 20/80 SBR/EVA

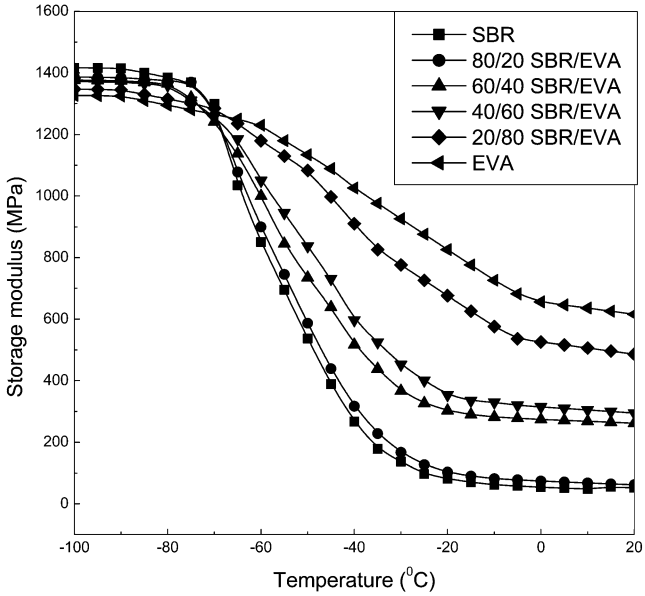

Fig. 3 Storage modulus of uncrosslinked SBR/EVA blends as a function of blend ratio and temperature (−100 to 20 °C) at a frequency of 1 Hz

temperature (−100 to 20 °C) are presented in Fig. 1. SBR displays a glass transition with highest damping value at −52 °C. The glass transition of EVA is around −17 °C with a damping value significantly lower than that observed for SBR. The lower damping value of EVA compared to SBR is associated with the semi-crystalline nature of the former.

Generally, for an incompatible blend, the tan δ vs. temperature curve shows the presence of two damping peaks corresponding to the glass transition temperatures of individual polymers [19]. For a highly compatible blend, the curve shows only a single peak [6] between the transition temperatures of the component polymers, where as a broadening of transition occurs in the case of partially compatible systems [20]. In the case of compatible and partially compatible blends, the T_gs are shifted to higher or lower temperatures as a function of composition. In the case of blends under investigation, two transitions corresponding to SBR and EVA phases are observed. The glass transition of SBR in the uncrosslinked blends did not change substantially indicating incompatibility. The peak intensity of the EVA phase is not so evident because of its low damping value. It is interesting to observe that the damping value increases gradually up to 40% of SBR followed by a more sharp increase from 40 to 60% of SBR. These results are in agreement with the results obtained from optical micrographic studies shown in Fig. 2, which indicated that when the EVA content is 50% or more, it forms a continuous phase. Similar behaviour has been reported in literature [21]. The increase in the damping and tan δ_{max} with increase in SBR content is due to the reduction in the crystallinity of the system upon increasing the concentration of SBR whose damping is always higher than EVA.

The variation of storage modulus of uncrosslinked components and blends in the temperature range of −100 to 20 °C at 1 Hz is presented in Fig. 3. It is seen that storage modulii decrease with increasing temperature due to the decrease in stiffness of the sample. The curves for all the components have the following three distinct regions: a glassy region, a transition region and a rubbery region. SBR has higher storage modulus than EVA below the T_g region, and the trend is reversed in the rubbery state. In the case of SBR, the storage modulus shows a drastic fall around the T_g region, while for EVA, the modulus drop is at a slower rate due to its crystalline nature. The higher modulus of SBR compared to EVA below the glass transition region is due to the fact that at this stage the entire molecular chains of amorphous SBR is completely frozen. As SBR undergoes transition from the fully glassy state to rubbery state, the storage modulus decreases considerably. In crystalline materials, during transition, only the amorphous part undergoes segmental motion, while the crystalline regions remain as solid until its melting temperature. Therefore in EVA, which is partially crystalline, the modulus drop happens only to a lesser extent than SBR. As in the case of blend components, the modulus of the blends decreases with increase in temperature. It can also be seen from the figure that the modulii of the blends decrease with increase in SBR content at a given temperature. At the glassy region, storage modulus becomes higher for the SBR rich blends and its values drop several times faster above T_g. This

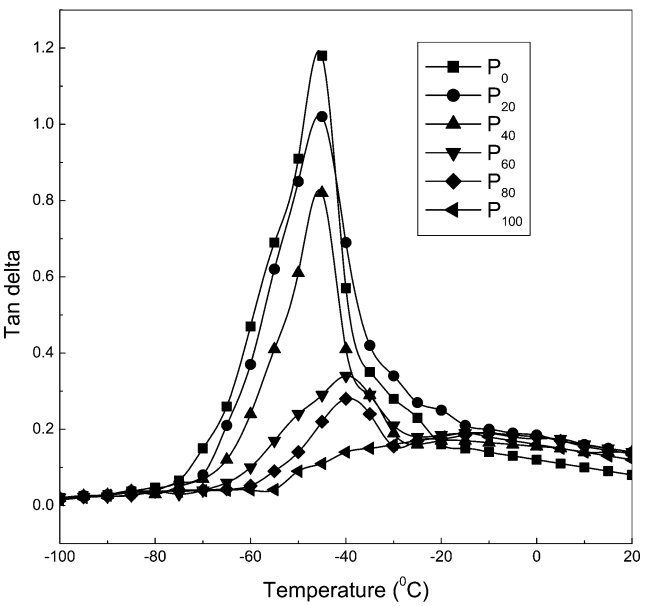

Fig. 4 Damping properties of DCP cured SBR/EVA blends as a function of blend ratio and temperature (−100 to 20 °C) at a frequency of 1 Hz

Table 3 T_g and tan δ_{max} of uncrosslinked and crosslinked SBR/EVA blends at 1 Hz

Sample code	SBR phase		EVA phase	
	tan δ_{max}	T_g (°C)	tan δ_{max}	T_g (°C)
SBR	1.38	−52.0	–	–
80/20 SBR/EVA	1.12	−52.0	–	–
60/40 SBR/EVA	0.89	−50.8	0.17	−18.0
40/60 SBR/EVA	0.45	−49.7	0.19	−17.4
20/80 SBR/EVA	0.33	−49.2	0.20	−17.0
EVA	–	–	0.21	−17.0
P_0	1.18	−46.0	–	–
P_{20}	1.02	−45.0	–	–
P_{40}	0.82	−43.0	0.17	−14.0
P_{60}	0.34	−41.0	0.18	−13.5
P_{80}	0.28	−40.0	0.19	−13.0
P_{100}	–	–	0.20	−14.0

behaviour is due to the better glass forming characteristics of SBR with a higher degree of modulus. Beyond the transition region, E' is higher for blends with lower SBR content. This is due to the influence of the crystalline regions of EVA.

The tan δ values of the peroxide cured homopolymers and blends as a function of temperature (−100 to 20 °C) at 1 Hz are shown in Fig. 4. The glass transition temperature of peroxide cured SBR (P_0) is −46 °C and that of EVA (P_{100}) is −14 °C. On comparing these T_g values with the corresponding T_g values of uncrosslinked polymers, it has been observed that the T_g of SBR is increased by 6 °C, whereas that of EVA is increased only by 3 °C. This could be due to the better crosslinking effect of DCP in SBR than EVA. The effect of blend composition on T_g and tan δ_{max} of uncrosslinked and peroxide cured SBR/EVA blends is presented in Table 3. In both uncrosslinked and peroxide cured blends, tan δ_{max} increases with increase in SBR content, i.e., the damping properties of the blends increase with increase in SBR content. The damping curves corresponding to SBR phase in DCP cured blends shifted towards higher temperature region upon increasing the EVA content. This indicates an enhanced interfacial adhesion between the components upon increasing the EVA content. Crosslinking enhances the T_gs of both the SBR and EVA phases due to the restriction in chain flexibility.

Effect of frequency

The dynamic mechanical properties of peroxide cured SBR/EVA blends were analyzed from −100 to 20 °C at different frequencies (0.1, 1, 10 and 50 Hz).The tan δ values of P_{60}

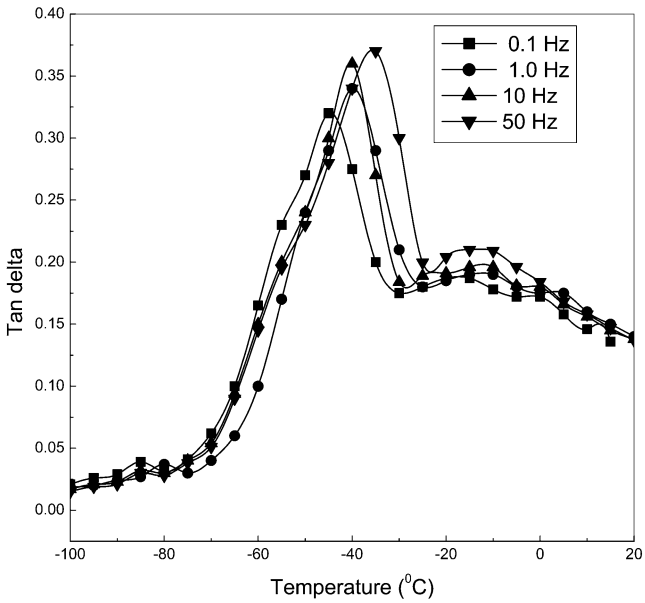

Fig. 5 Damping properties of P_{60} as a function of temperature and frequency

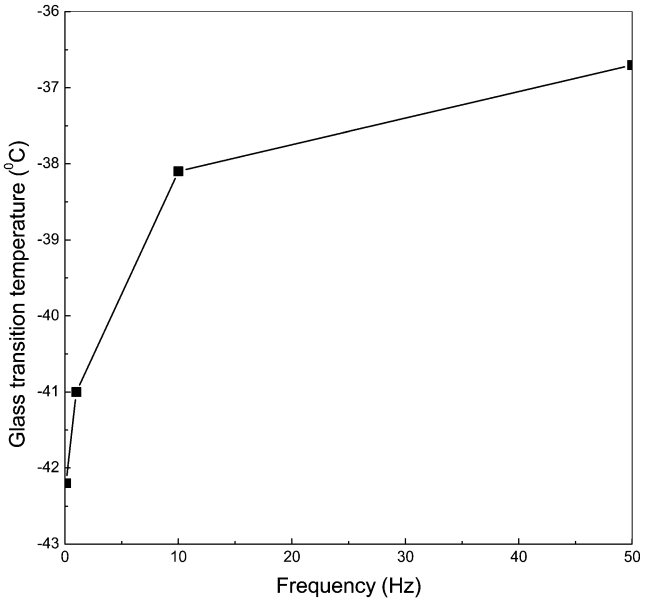

Fig. 6 Effect of frequency on glass transition temperature of SBR phase in P_{60}

Table 4 Effect of blend composition and frequency on T_g (°C) values (from tan δ peak)

Frequency (Hz)	Blend composition				
	P_0	P_{20}	P_{40}	P_{60}	P_{80}
0.1	−47.1	−46.2	−45.4	−42.2	−41.6
1.0	−46	−45	−43	−41	−40
10.0	−44	−43.2	−41.1	−38.1	−37.7
50.0	−38.6	−39	−38.5	−36.7	−34.9

at different frequencies as a function of temperature are given in Fig. 5. The glass transition temperatures of SBR and EVA phases are shifted towards the high temperature region with increasing frequency. This is also evident from Fig. 6, where the glass transition temperature of SBR phase in P_{60} is plotted against frequency. The effects of blend composition and frequency on glass transition temperature obtained from tan δ peak of peroxide cured blends are presented in Table 4.

The activation energy, E, for the glass transition of SBR phase in peroxide cured SBR/EVA blends has been calculated from Arrhenius relationship:

$$X = X_0 \exp[-E/RT] \quad (5)$$

Here X is the experimental frequency, X_0, a constant, and T is the temperature corresponding to the maximum of the tan δ curve. The activation energy values for the glass transition of SBR phase in various peroxide cured SBR/EVA blends are given in Table 5. The E value has been found to increase with increase in EVA content in the blends up to 60% of EVA. This is due to the enhanced interfacial adhesion between the blend components. However, the activation energy decreases with increase in EVA content from 60% to 80%. This has been due to the decrease in adhesion at the interface, which resulted in coalescence and an increased domain size.

The variation of storage modulus with temperature of P_{60} at different frequencies is given in Fig. 7. Here also the three distinct regions for the glassy, transition and rubbery regions are evident. In the glassy region, the blends exhibit almost similar modulii at all frequencies, whereas in the transition and rubbery regions there is a marginal increase in modulus with increasing frequency.

Table 5 Arrhenius activation energy for glass transition of SBR phase in peroxide cured SBR/EVA blends

Sample code	E (kJ/mol)
P_0	125.83
P_{20}	154.61
P_{40}	177.63
P_{60}	207.74
P_{80}	182.17

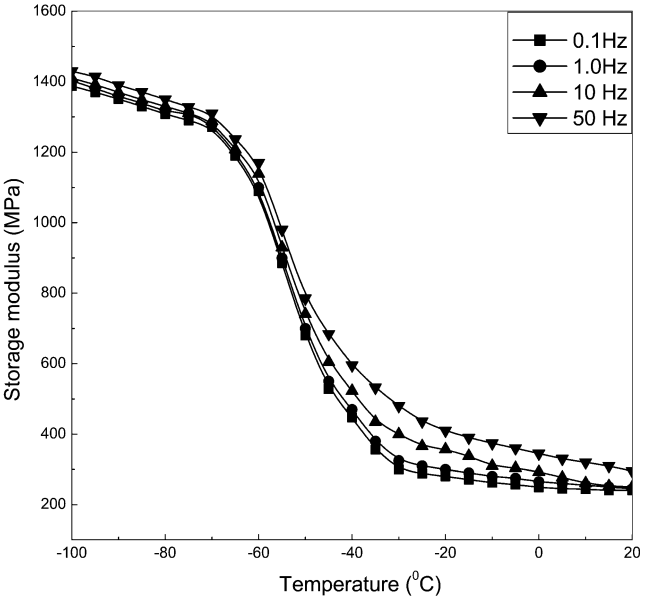

Fig. 7 Storage modulus of P_{60} as a function of temperature and frequency

Effect of crosslink density

Properties of elastomers are largely dependent on the crosslinks introduced between the macromolecular chains. Therefore, it is important to examine the effect of crosslink densities on the dynamic mechanical properties. Figure 8 shows the dependence of tan δ on temperature for uncrosslinked and various crosslinked 40/60 SBR/EVA systems, at 1 Hz. All

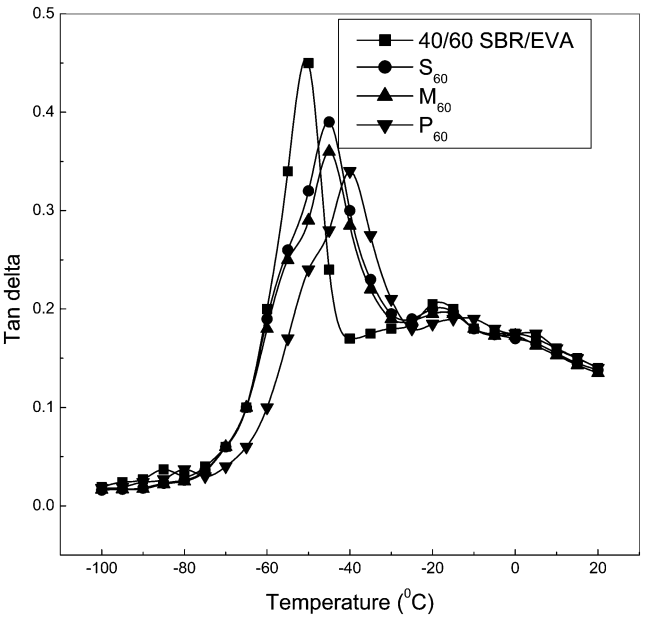

Fig. 8 Damping properties of 40/60 SBR/EVA blends as a function of temperature and crosslinking systems at a frequency of 1 Hz

the blends present two damping peaks, confirming the incompatibility of the components. The vulcanization with sulphur, DCP and mixed (*S*+DCP) systems shifts the glass transition temperature of SBR phase towards higher values. These features are related to the decrease in the molecular mobility of this phase, as a consequence of crosslinking. The crosslink densities of the samples were determined by the swelling method [17]. The degree of crosslinks has been calculated by the equation [22]

$$\nu = \frac{1}{2M_c} \tag{6}$$

where M_c is the molar mass between crosslinks. Molar mass between the crosslinks of the samples has been calculated from the Flory–Rehner equation [23].

$$M_c = \frac{-\rho_p V_s \phi^{1/3}}{\left[\ln(1-\phi) + \phi + \chi\phi^2\right]} \tag{7}$$

where ρ_p is the density of the blend, V_s, the molar volume of the solvent and ϕ, the volume fraction of blend in the swollen sample. The ϕ has been determined by the method reported by Ellis and Welding [24]

$$\phi = \frac{(d - fw)\rho_p^{-1}}{(d - fw)\rho_p^{-1} + A_0\rho_s^{-1}} \tag{8}$$

where d is the deswollen weight of the sample, w the initial weight of the sample, A_0, the weight of the solvent in the swollen sample, f the fraction of insoluble component, ρ_p and ρ_s, the densities of the blend and solvent, respectively.

χ is the polymer-solvent interaction parameter. It has been calculated by the expression [25]

$$\chi = \frac{(\mathrm{d}\phi/\mathrm{d}t)\{[\phi/1-\phi] + N\ln(1-\phi) + N\phi\}}{2\phi(\mathrm{d}\phi/\mathrm{d}T) - \phi^2 N(\mathrm{d}\phi/\mathrm{d}T) - \phi^2/T} \tag{9}$$

N has been calculated from ϕ as follows:

$$N = \frac{\left[\phi^{2/3}/3 - 2/3\right]}{\left[\phi^{2/3} - 2\phi/3\right]} \tag{10}$$

The values of tan δ_{max}, T_g of SBR phase at 1 Hz and crosslink density (ν) for 40/60 SBR/EVA systems are given in Table 6. The damping peak height increases in the order: 40/60 SBR/EVA>S_{60}>M_{60}>P_{60}. This is in the order of increasing crosslink density.

Table 6 Values of tan δ_{max}, T_g and ν for uncrosslinked and crosslinked 40/60 SBR/EVA at 1 Hz

Sample code	tan δ_{max}	T_g of SBR phase	Crosslink density, ν (kg mol/m^3)
40/60 SBR/EVA	0.45	−49.7	–
S_{60}	0.39	−45	9.67×10^{-2}
M_{60}	0.36	−43.5	9.84×10^{-2}
P_{60}	0.34	−41	18.70×10^{-2}

The variations of storage modulus of various crosslinked 40/60 SBR/EVA systems are presented in Fig. 9. The modulus value is lowest for sulphur crosslinked systems which is having the lowest crosslink density and highest for peroxide cured system which has the highest crosslink density.

Effect of compatibilization

The addition of the compatibilizer, SEBS-g-MA, has been found to improve the mechanical properties of SBR/EVA blends significantly [18]. Prior to compatibilization, the blend is characterized by a sharp interface due to the higher interfacial tension and poor adhesion between the components, which in turn is due to the differences in the chemical constitution of the component polymers. The compatibilizer located at the interface, reduces the interfacial tension, helps to develop a finer dispersion and, thus prevents the tendency against gross segregation. As a result, systems with improved and reproducible properties are obtained. The morphology of uncompatibilized and compatibilized SBR/EVA blends, attested by the SEM photographs given in Fig. 10 supports these observations. The gray region corresponds to SBR phase, which was stained by OsO_4 and the dark regions belong to the unstained EVA phase. Figure 10(a) shows the micrographs of peroxide cured uncompatibilized 40/60 SBR/EVA blend system, where SBR was found to be dispersed as domain in continuous EVA phase. Compatibilization of this system resulted in a decrease

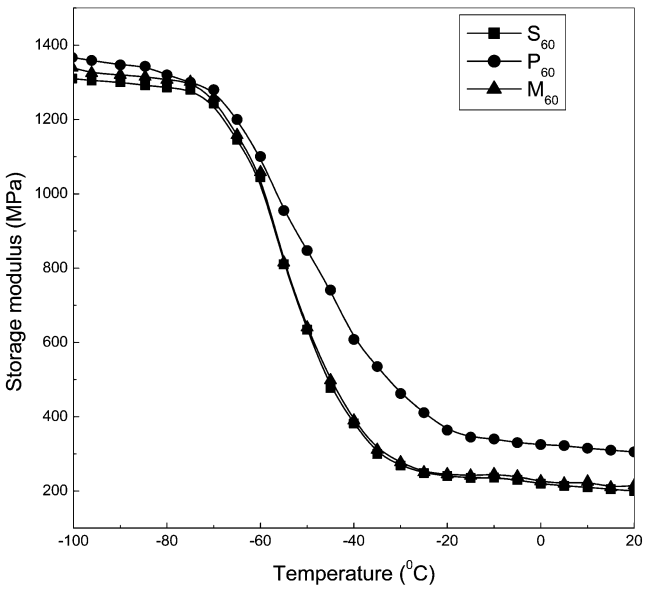

Fig. 9 Storage modulus of 40/60 SBR/EVA blends as a function of temperature and crosslinking systems at a frequency of 1 Hz

in the domain size as shown by Fig. 10(b). This is due to the decreased interfacial tension provided by the compatibilizer.

The variation of tan δ as a function of temperature, of peroxide cured uncompatibilized and compatibilized 40/60 SBR/EVA blends with 6 phr SEBS-g-MA, at 1 Hz is presented in Fig. 11. The compatibilized blends also show the same behaviour for the tan δ curve as that of the unmodified blends, i.e. they show the presence of two maxima corresponding to the glass transition temperatures of SBR and EVA. However, there is a small decrease and broadening of the damping peak related to SBR and EVA phases, in the compatibilized systems, indicating the increase in interfacial interaction which leads to a decrease in segmental motion.

Figure 12 depicts the variation of storage modulus of peroxide cured uncompatibilized and compatibilized 40/60 SBR/EVA blends with 6 phr SEBS-g-MA with temperature at 1 Hz. With the addition of 6 phr compatibilizer, the storage modulus is slightly enhanced at all temperatures. This is due to the increase in the interfacial adhesion caused by the compatibilizer, which results in a more homogeneous morphology. The reduction in particle size with the addition of compatibilizer is due to the reduction in the interfacial tension between the dispersed SBR and EVA phases.

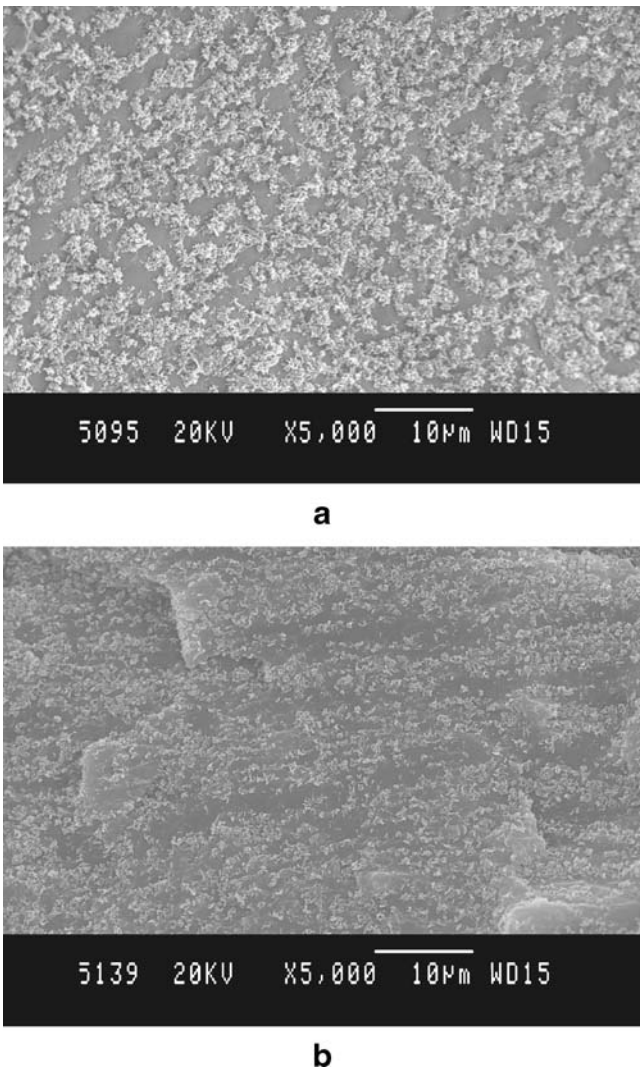

Fig. 10 SEM photographs of DCP cured uncompatibilized and compatibilized 40/60 SBR/EVA blends (**a**) P_{60} and (**b**) $P_{60}C_6$

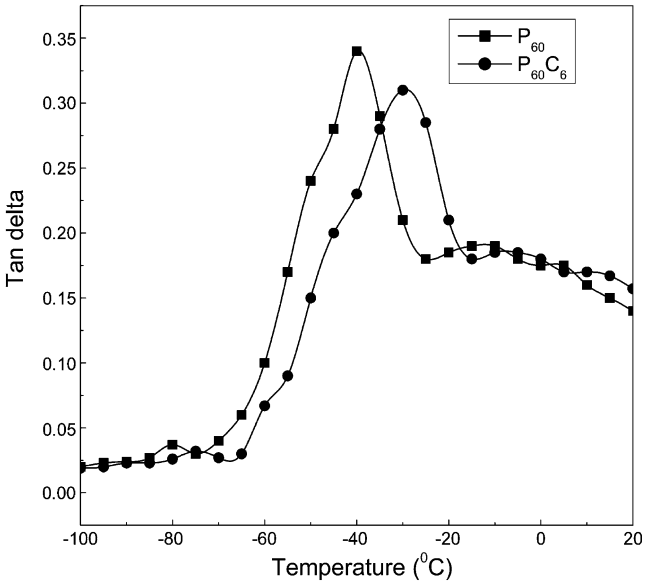

Fig. 11 Variation of tan δ of uncompatibilized and compatibilized, peroxide cured 40/60 SBR/EVA blends

Theoretical modelling

To assess the behaviour of the two-phase blends from the DMA data, different theoretical models have been used.

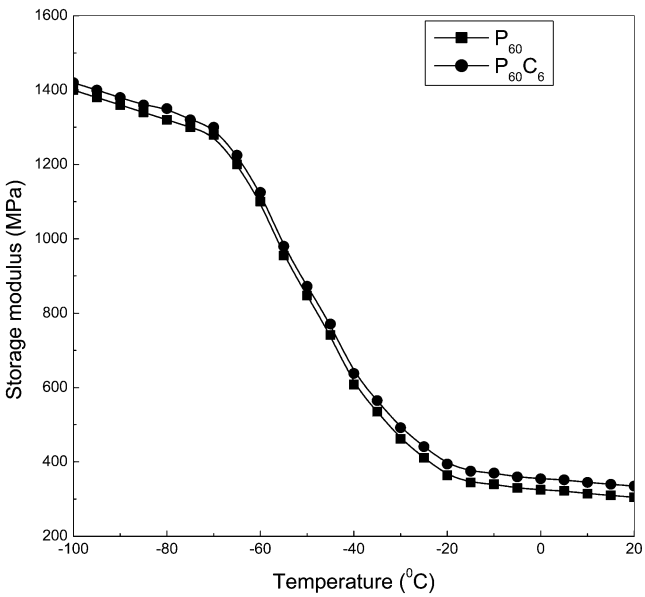

Fig. 12 Variation of storage modulus of uncompatibilized and compatibilized, peroxide cured 40/60 SBR/EVA blends

The various models applied include parallel, series, Halpin–Tsai and Coran's.

The parallel model (highest upper bound model) is given by the equation, [20]

$$M = M_1\phi_1 + M_2\phi_2 \tag{11}$$

where M is the property of the blend, M_1 and M_2 are the properties of the components 1 and 2 respectively, ϕ_1 and ϕ_2 are the volume fractions of the components 1 and 2, respectively. In this model, the components are considered to be arranged parallel to one another so that the applied stress elongates each of the components by the same extent.

In the lowest lower bound series model, the components are arranged in series with the applied stress. The equation [20] is,

$$1/M = \phi_1/M_1 + \phi_2/M_2 \tag{12}$$

According to the Halpin–Tsai equation, [26]

$$M_1/M = (1 + A_iB_i\phi_2)/(1 - B_i\phi_2) \tag{13}$$

where

$$B_i = (M_1/M_2 - 1)/(M_1/M_2 + A_i) \tag{14}$$

In these equations, the subscripts 1 and 2 refer to the continuous and dispersed phases respectively. The constant A_i is defined by the morphology of the system. A_i=0.66 when a flexible component forms the dispersed phase in a continuous hard matrix. On the other hand, if the hard material forms the dispersed phase in a continuous flexible matrix, A_i=1.5.

In Coran' s model, the properties are generally in between the upper bound parallel model (M_U) and the lower bound series model (M_L).

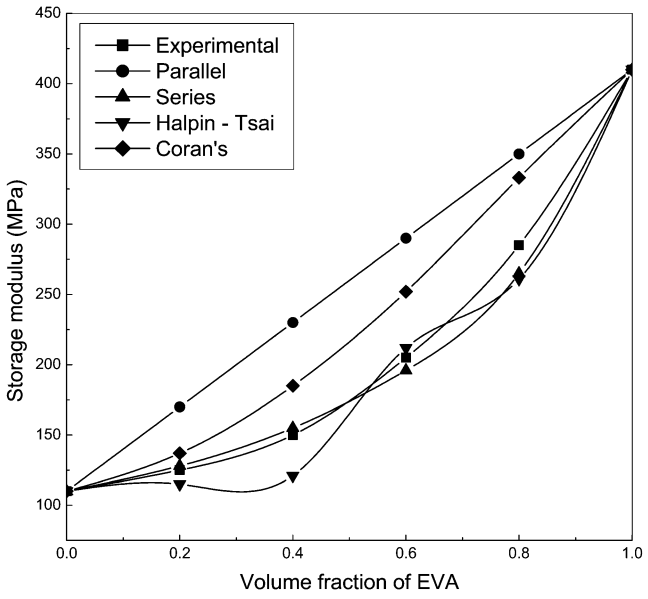

Fig. 13 Experimental and theoretical curves of storage modulus of DCP cured SBR/EVA blends

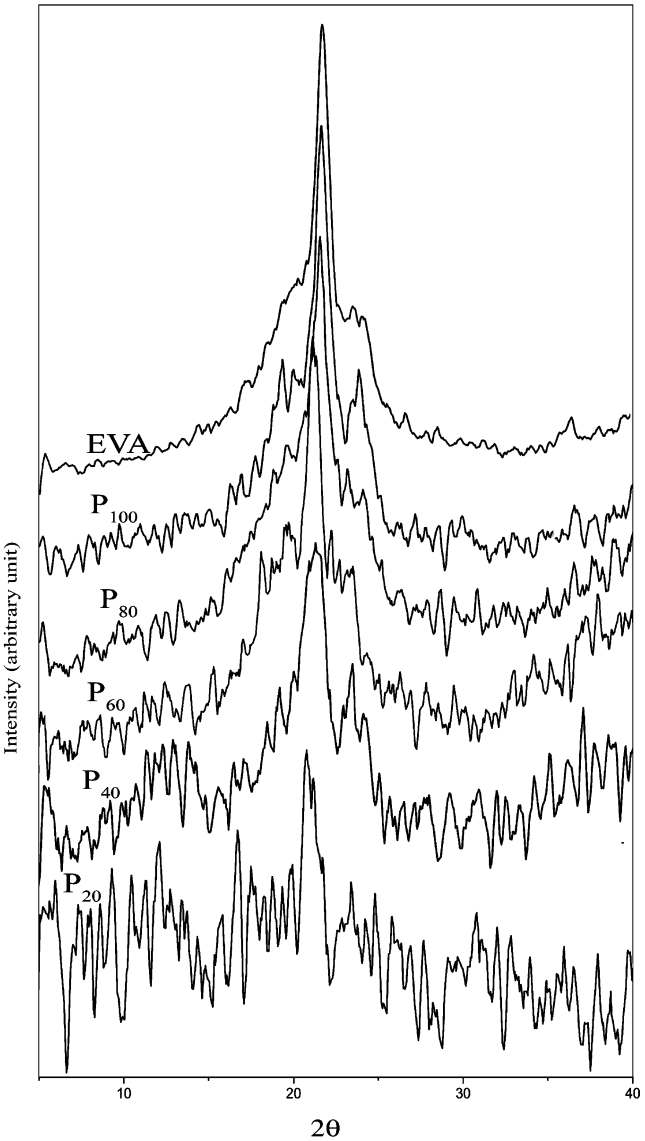

Fig. 14 X-ray diffraction patterns of EVA and peroxide cured SBR/EVA blends

Table 7 Crystallinity of SBR/EVA blends

Sample	Degree of crystallinity, X_C (%)
EVA	34.5
P_{100}	32.4
P_{80}	25.8
P_{60}	19.5
P_{40}	12.4
P_{20}	6.5

According to Coran's equation, [27]

$$M = f(M_U - M_L) + M_L \quad (15)$$

where f varies between 0 and 1. The value of f is a function of phase morphology and is given by

$$f = V_H^n(nV_s + 1) \quad (16)$$

where n is related to phase morphology, V_H and V_S are the volume fractions of hard and soft phases respectively.

The storage modulus of peroxide cured SBR/EVA blends was calculated applying Equations 11 to 16. The curves resulting from the theoretical models and that of the experimental data, for the variation of storage modulus at 30 °C with the volume fraction of EVA, are given in Fig. 13. The experimental data has been found to fit well with the series model. The parallel model and Coran's model show the upper bound over the entire compositions.

X-ray diffraction studies

The crystallinity of uncrosslinked EVA and crosslinked SBR/EVA blends were investigated by using wide angle X-ray scattering. The X-ray diffraction patterns of the uncrosslinked EVA and peroxide cured blends are given in Fig. 14. Results of the X-ray analysis of the samples are given in Table 7. The degree of crystallinity decreases with an increase in the SBR content. This is due to the migration of the amorphous component, SBR, to the crystalline phase of pure EVA. The introduction of crosslinks further reduces the crystallinity of the system. This is due to the fact that the crosslinks hinder the regular arrangement of the crystalline regions within the sample.

Conclusion

The DMA of SBR/EVA blends has been carried out as a function of blend composition, crosslinking systems and compatibilization over a wide range of temperature and frequency. The two separate tan δ peaks, obtained during DMA, indicated that SBR/EVA system was immiscible. As the EVA content in the blends increased, the storage modulus increased, while tan δ decreased. The tan δ peak corresponding to SBR component shifted slightly towards higher temperature region upon increasing the EVA content in the blend, which showed the enhanced interaction between the components. The glass transition temperature (T_g) was shifted towards the higher temperature region with increase in frequency. The damping characteristics of the blends were affected by the variations in frequency. The T_gs of the blends were shifted towards the higher temperature, while tan δ_{max} decreased with an increase in crosslink density. The activation energy for glass transition of SBR phase in peroxide cured blends increased with an increase in EVA content up to 60% of EVA. This has been due to enhanced interfacial adhesion between the blend components. The presence of the compatibilizer resulted in a small decrease and a broadening of the damping peak related to SBR phase, showing an increased interfacial interaction. The addition of the compatibilizer has been found to increase the storage modulus and reduced damping properties. The experimental results of storage modulus have been found to fit well with series model.

References

1. Murayama T (1977) Dynamic mechanical analysis of polymeric materials. Elsevier, New York
2. Kevin PM (1999) Dynamic mechanical analysis – a practical introduction. CRC Press, New York
3. Read BE, Brown GD (1978) The determination of the dynamic properties of polymers and composites. Wiley, New York
4. Ferry J (1980) Viscoelastic properties of polymers, 3rd edn. Wiley, New York
5. Karger-Kocsis J, Kiss L (1987) Polym Eng Sci 27:254
6. Khonakdar HA, Wagenknecht U, Jafari SH, Hassler R, Eslami H (2004) Adv Polym Technol 23:307
7. Omonov TS, Harrats C, Moussaif N, Groeninckx G, Sadykov SG, Ashurov NR (2004) J Appl Polym Sci 94:2538
8. Jansen P, Soares BG (2002) J Appl Polym Sci 84:2335
9. Wu C, Akiyama S (2001) Polym J 33:955
10. Oommen Z, Groeninckx G, Thomas S (2000) J Polym Sci Part B Polym Phys 38:525
11. Pandey KN, Setua DK, Mathur GN (2005) Polym Eng Sci 45:1265
12. Hamdan S, Hashim DMA, Ahmad M, Embong S (2000) J Polym Res 7:237
13. Kader MA, Kim WD, Kaang S, Nah C (2005) Polym Int 54:120
14. Brahimi B, Ait-Kadi A, Ajji A, Fayt R (1991) J Polym Sci Part B Polym Phys 29:945
15. Li Y, Williams HL (1990) J Appl Polym Sci 40:1881
16. Radhakrishnan CK, Sujith A, Unnikrishnan G, Thomas S (2004) J Appl Polym Sci 94:827
17. Radhakrishnan CK, Ganesh B, Sujith A, Unnikrishnan G, Thomas S (2005) Polym Polym Compos 13:335
18. Radhakrishnan CK, Rosamma A, Unnikrishnan G (2006) Polym Degrad Stab 91:902
19. Gonzalez-Montiel A, Keskkula H, Paul DR (1995) Polymer 36:4587
20. Thomas S, George A (1992) Eur Polym J 28:1451
21. Koshy AT, Kuriakose B, Thomas S, Varghese S (1993) Polymer 34:3428
22. Bristow GM, Watson WF (1958) Trans Faraday Soc 54:1731
23. Flory PJ, Rehner J Jr (1943) J Chem Phys 11:521
24. Ellis B, Welding GN (1964) Techniques in polymer science. Society of the Chemical Industry, London
25. Khinnavar RS, Aminabhavi TM (1991) J Appl Polym Sci 42:2321
26. Nielson LE (1974) Rheol Acta 13:86
27. Coran AY (1998) In: Bhowmick AK, Stephens HL (eds) Hand book of elastomers, new developments and technology. Marcel Dekker, New York, p 249